On the Electromagnetic Pulse Produced by Nuclear Explosions

CONRAD L. LONGMIRE

Abstract—The electromagnetic pulse (EMP) produced by the gamma rays from nuclear explosions is discussed. The gamma rays produce a current of Compton recoil electrons, and these electrons produce further ionization so that the air becomes conducting. The Compton current leads to the generation of electromagnetic fields according to Maxwell's equations. The conductivity tends to limit the magnitude of the fields. Approximate methods of solving the equations are described by considering time regimes in which various terms in the equations are negligible, e.g., either the conduction current or the displacement current can be dropped. Further advantage is obtained by replacing the transverse fields by outgoing and ingoing waves; outgoing waves are dominant at early times. Features of the solutions are described for nuclear bursts at the ground surface and at high altitude. The history of EMP is reviewed briefly.

I. INTRODUCTION

NUCLEAR EXPLOSIONS in or above the earth's atmosphere produce an electromagnetic pulse (EMP) by several mechanisms, of which the most important is perhaps the gamma-ray mechanism. The nuclear explosion produces an intense pulse of gammas, with a rise time of the order of a few nanoseconds (ns). The gammas, in traveling through the air, produce a flux of Compton recoil electrons that constitutes an electric current density with a rise time of the same order. This current density generates the EMP according to Maxwell's equations. The frequency content of the EMP extends up to frequencies corresponding to the current rise time.

Each of the Compton recoil electrons, which have starting energies of the order of 1 MeV, generates of the order of 30 000 secondary electron-ion pairs along its track in the air. The secondary electrons and ions make no appreciable electric current at birth compared with the Compton current, but they will drift in the presence of an electric field; thus they make an electrical conductivity. This conductivity is an important factor in limiting the amplitude and determining the waveform of the EMP.

Since the gammas move outward from the burst at the velocity of light, the Compton current pulse also appears to do so. This traveling-pulse feature of the Compton current has a strong effect on the EMP: EM signals generated at different distances from the burst, and therefore at different times, tend to arrive simultaneously at a more distant observer on the same ray. This is the same effect as that obtained from a phased array antenna. The space-time phasing of the Compton current is such as to put more energy in outgoing waves than ingoing, particularly for the high-frequency content.

The asymmetries of the gamma source and the surrounding medium are obviously also important. For instance, a spherically symmetric distribution of radial Compton current can produce only a spherically symmetric radial (longitudinal) electric field with no magnetic or radiated (transverse) fields. Important asymmetries which lead to the production of transverse fields include the air-ground interface, the atmospheric density gradient, and the geomagnetic field through its deflection of the Compton recoil electrons.

This paper will review the physics of the gamma source, the Compton current, the air conductivity, and the generation of the fields for the gamma-ray mechanism. In the space available it will not be possible to review thoroughly the work of the many contributors to the total development of EMP theory and calculations. The author has chosen to review the salient physical concepts and results, and to focus the references on the historical development of EMP, a task not previously accomplished in the open literature. The reader wishing to make more complete contact with the literature can make use of the extensive EMP note series compiled and distributed by the Air Force Weapons Laboratory (AFWL) through the heroic efforts of Carl E. Baum, or the extensive EMP information in the nuclear effects library maintained by the Defense Nuclear Agency (DNA).

II. THE GAMMA SOURCE

We shall first consider a nuclear explosion in the air just above the ground surface (*surface burst*). A hypothetical but not atypical example of the gamma [1] source strength from a 1-megaton surface burst is shown in Fig. 1. The total source is the sum of several components, each with its characteristic decay time. *Prompt gammas* come out of the nuclear device, have a rise time of a few nanoseconds, and decay in a few tens of nanoseconds. The other gammas are made by neutrons that leave the device and interact with the air and ground. Fast neutrons striking solid objects (e.g., the ground) very near the device make *inelastic scatter gammas* in the same time frame as the prompt gammas. Fast neutrons (energy $\gtrsim$ 6 MeV) make *air inelastic gammas* by inelastic scattering in air. *Ground capture gammas* are made by neutrons that slow down and get captured in the ground. *Air capture gammas*, made by the same process in air, last longer because of the low density of air compared with ground. *Fission product gammas*, the longest lived source, are emitted by fission debris following the lingering beta decay of fission fragments.

Manuscript received September 24, 1976; revised June 28, 1977.
The author is with Mission Research Corporation, Santa Barbara, CA 93102.

0018-926X/78/0100-0003$00.75

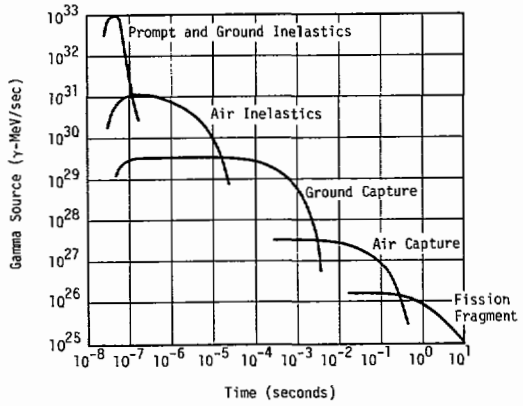

Fig. 1. Total gamma source strength versus time for nominal 1-megaton surface burst.

For a burst somewhat above the ground, some time is required for the neutrons to reach the ground so that ground inelastic and capture sources are delayed somewhat. At increasing burst altitudes the intensities of the air inelastic and air capture sources decrease, and their lifetimes increase due to decreasing air density. For bursts at very high altitudes, the ground sources are absent and the air sources are delayed until neutrons can reach the sensible atmosphere at altitudes of the order of 30 km. The speed of the fastest neutrons is about 50 km/ms (millisecond).

While the prompt gamma source can be regarded as a point source, the volumes of the air and ground sources obviously depend on burst geometry. In sea level air, neutron mean free paths are of the order of 100 m, and the air sources have dimensions of a few mean free paths.

Approximate average gamma-ray energies and effective absorption lengths in the air are listed in Table I for the various sources. Estimates of the gamma flux F_γ at distance r from the burst can be made by using spherical dilution and attenuation factors, e.g., in uniform air

$$F_\gamma \sim e^{-r/\lambda_a}/4\pi r^2 \tag{1}$$

where λ_a is the effective absorption length in length units. Gamma scattering causes some but not overwhelming change in the time dependence of the gamma flux at distance as compared with the source form. Quite satisfactory analytical expressions for the gamma flux can be obtained by fitting formulas like (1), with simple build-up factors, to the results of Monte Carlo calculations.

III. THE COMPTON CURRENT

In the Compton scattering process [1] an incident gamma is scattered by an atomic electron, and the electron recoils somewhat like a struck billiard ball. The angular distribution of the recoil electrons peaks in the forward direction so that a net electric current results. The average kinetic energy of the recoil electrons is of the order of one-half the incident gamma energy.

As the recoil electrons move through the air or other material medium they gradually lose energy to other atomic electrons

TABLE I
APPROXIMATE AVERAGE ENERGIES AND EFFECTIVE ABSORPTION LENGTHS IN AIR OF GAMMA SOURCE COMPONENTS

Component	Energy, MeV	Absorption length, gm/cm^2
prompt	1.5	40
air inelastic	4	52
ground capture	3	38
air capture	6	58
fission fragment	1	37

with which they collide, dislodging some from their atoms and thus producing ionization. The energy loss is sufficient to bring the recoil electron to rest within a distance (*track length*) of a few meters in sea level air. In addition, the recoil electrons suffer many small-angle scatterings (*multiple scattering*), largely in collisions with atomic nuclei. The multiple scattering reduces the *mean forward range* of recoil electrons to about two-thirds of the track length.

The geomagnetic field deflects the Compton recoil electrons, leading to components of Compton current in directions other than the direction of the incident gammas. This effect is relatively small at sea level as the *Larmor radius* of the recoil electrons in the geomagnetic field is 50 to 100 m, which is long compared with the mean forward range at sea level. However, at a 30-km altitude, the center of the *source region* for high-altitude EMP, the mean forward range is comparable with the Larmor radius. Thus the deflected (transverse) Compton current is comparable with the radial current and is the principle source of the high-altitude EMP. Even for low-altitude bursts the geomagnetic effect is significant, especially for the high-frequency part of the EMP from air bursts where the strong asymmetry due to the ground is not present.

The Compton recoil electrons are also affected by the EMP fields. EMP calculations which include this effect are called *self-consistent* since the fields are allowed to affect the Compton current which produces the fields. Such calculations are nonlinear and are performed on electronic computers.

A simple computer scheme for calculating the Compton currents was developed by Longmire and Longley [2], [3]. At each time step a set of sample Compton recoil electrons is started off, with weight factors proportional to the gamma flux and the proper angular distribution. Equations of motion of the recoil electrons are solved forward in time, with the forces from the geomagnetic and the instantaneous EMP fields included. Energy loss to ionization is treated by adding a *drag force* which, in the case of zero fields, would stop the electron in the correct track length. Multiple scattering is treated by defining a mean *obliquity factor*

$$\eta = \frac{1}{\cos\theta} \approx 1 + \frac{\theta^2}{2}. \tag{2}$$

Here θ^2 is the mean squared angle of deviation of the trajectories of multiply scattered electrons relative to the trajectory of an unscattered electron. Simple multiple scattering theory is used to determine how θ^2, and therefore η, increases with time. It is then assumed that the mean velocity of the "cloud" of scattered electrons is reduced by a factor η with respect to

that of an unscattered electron; the reduced velocity is used in computing the Compton current density.

The drag force and obliquity factor method is obviously only a first approximation to the effects of energy loss and multiple scattering. Longmire and Longley showed that it accounts quite well for experimental data on the transmission of electron beams through aluminum foils. Knutson [4] compared its results with results obtained by him using a Monte Carlo treatment of the multiple scattering (a much more time consuming method), and found agreement within a few percent over the main contribution to the Compton current. Vajk [5] has studied the effect of fluctuations in energy loss (*straggling*) on the Compton current, also by a Monte Carlo method. However, there are inconsistencies in his results in that the initial value of his radial Compton current disagrees with that obtained by other methods; this value cannot be affected by the energy loss and scattering model. There can be little doubt that the drag force and obliquity factor method is adequate in most practical cases.

It is easy to understand the general magnitude of the Compton current. A steady flux F_γ of collimated gammas will produce a steady flux of recoil electrons in the same direction according to the relation

$$F_e = F_\gamma \frac{R_{mf}}{\lambda_s} \approx 0.007 F_\gamma \tag{3}$$

where λ_s is the scattering mean free path of the gammas and R_{mf} is the mean forward range of the recoil electron. A *dose rate* of 1 rad/s corresponds to a gamma flux of about 2×10^9 gamma-MeV/cm^2 s. Thus in terms of the dose rate $\dot{D}$, the radial Compton current density J_r is

$$J_r \left(\frac{\text{A}}{\text{m}^2} \right) \approx 2 \times 10^{-8} \dot{D} \left(\frac{\text{rad}}{\text{s}} \right). \tag{4}$$

This formula is valid from sea level up to about a 30-km altitude where the geomagnetic field limits the mean forward range. The transverse geomagnetically deflected Compton current density is

$$J_t \approx J_r \frac{R_{mf}}{2R_L} \tag{5}$$

where R_L is the *Larmor radius*. J_t and J_r are comparable at a 30-km altitude.

At sea level the effective lifetime (before stopping) of a Compton recoil electron is a few nanoseconds. Thus the waveform of the Compton current will be approximately the same as that of the gamma flux. At a 30-km altitude the lifetime is about 1 μs, as is also the Larmor period. Here the current waveform is streched by recoil electron dynamics in the early part of the gamma pulse. Fig. 2 shows typical radial and transverse currents for a very short (delta-function) pulse of gammas. The currents are plotted as functions of *retarded time* τ

$$\tau = t - \frac{r}{c} \tag{6}$$

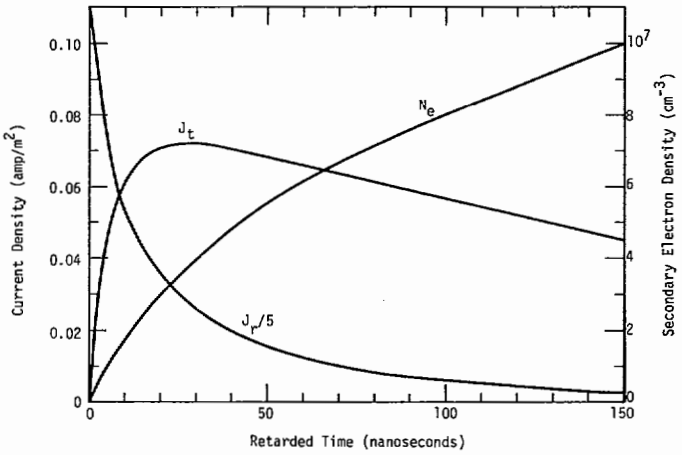

Fig. 2. Radial and transverse Compton currents J_r and J_t, and secondary electron density N_e versus retarded time at 31.4-km altitude for delta-function pulse of 4.62×10^9 1.5 MeV gammas per cm^2, perpendicular to geomagnetic field of 0.6 G.

for convenience in understanding the solution of Maxwell's equations. Note that if a recoil electron starting at $t = 0$ moved outwards with speed c (the speed of light) its retarded time would remain equal to zero. The fact that the recoil electrons do move outwards with speeds close to c accounts for the relatively large amplitude of J_r and J_t at early retarded times.

IV. THE AIR CONDUCTIVITY

A Compton recoil electron makes approximately one secondary electron-ion pair for each 85 eV lost by it in collisions with atoms. Most of the secondary electrons have energies of the order of 10 eV, but a few have larger energies approaching one-half that of the original electron. The more energetic secondary electrons produce tertiaries, etc. When all the ionization is completed there is approximately one electron-ion pair for each 34 eV lost by the original Compton recoil electron. Thus a 1-MeV electron will produce eventually about 30 000 electron-ion pairs.

The time dependence of the buildup of ionization density after passage of an energetic electron was calculated by Longmire and Koppel [6]. At sea level, ionization is 90 percent completed by 1 ns after passage; at a 30-km altitude the time required is about 50 ns.

The 10-eV electrons cool further by collisions with air molecules; they would eventually reach the same temperature as the air if there were no electric field present. Baum [7] has calculated the time dependence of this cooling. At sea level the time to thermalize is about 2 ns, while at a 30-km altitude it is about 100 ns. The actual final temperature depends on the electric field since Joule heating raises the equilibrium temperature of the drifting electrons. Times to reach equilibrium [7] are usually much less than the numbers mentioned.

Both electrons and ions contribute to the conductivity, so that it is necessary to keep track of their densities. Free electrons are removed predominantly by the *attachment* process

$$e + O_2 + O_2 \rightarrow O_2^- + O_2 \tag{7}$$

which produces the negative oxygen ion. At very high electron and ion densities, *dissociative recombination* removes both electrons and positive ions

$$e + O_2^+ \rightarrow O + O$$
$$e + N_2^+ \rightarrow N + N. \tag{8}$$

Positive and negative ions remove each other by *mutual neutralization* with the help of a third molecule M (either O_2 or N_2)

$$O_2^- + O_2^+ + M \rightarrow O_2 + O_2 + M$$
$$O_2^- + N_2^+ + M \rightarrow O_2 + N_2 + M. \tag{9}$$

Both O_2^+ and N_2^+ are produced, along with e, in the original ionization. Since the conductivity properties of O_2^+ and N_2^+ are nearly the same, it is not necessary to keep track of both species separately. The common treatment defines densities N_e, N_+, and N_- of electrons and positive and negative ions, respectively, which satisfy the differential equations

$$\frac{dN_e}{dt} = S - k_1 N_e - k_2 N_e N_+$$
$$\frac{dN_+}{dt} = S - k_2 N_e N_+ - k_3 N_+ N_-$$
$$\frac{dN_-}{dt} = k_1 N_e - k_3 N_+ N_-. \tag{10}$$

Here S is the rate of production of electron-ion pairs. It is easily verified that these equations conserve charge, i.e., $N_+ - N_e - N_-$, remains zero if initially zero. The effect of drift (transport) has been neglected as in the usual quasi-neutral plasma approximation. This approximation is valid in most EMP applications. However, boundary layers that form near metal or other solid surfaces, due to the fact that conduction electrons cannot flow out of the surface, are sometimes important. The rate constants k_1, k_2, k_3 are for the reactions (7), (8), and (9), respectively. Typical values of these constants at sea level and their scaling with air density ρ are

$$k_1 \approx 10^8/\text{s}, \qquad k_1 \sim \rho^2$$
$$k_2 \approx 2 \times 10^{-7}\ \text{cm}^3/\text{s}, \qquad \text{independent of } \rho$$
$$k_3 \approx 2 \times 10^{-6}\ \text{cm}^3/\text{s}, \qquad k_3 \sim \rho. \tag{11}$$

The value of k_1 is affected by the presence of an electric field [8]. Also, the complete recombination chemistry is somewhat more complicated than described here, especially in the presence of water vapor [9].

Simple approximate solutions to (10) are often useful. For example, the reaction (8) is usually negligible compared with (7). Then, for an ionization source S which changes slowly compared with k_1, the electron density is approximately

$$N_e \approx S/k_1. \tag{12}$$

For a source which rises exponentially, $S \sim e^{\alpha t}$ (as for fission chain reactions), the solution is

$$N_e = S/(\alpha + k_1). \tag{13}$$

For a source which falls more slowly than t^{-2}, the late-time ion densities are

$$N_- \approx N_+ \approx \sqrt{S/k_3}. \tag{14}$$

Finally, for a source which falls more rapidly than t^{-2}, the late-time ion densities are

$$N_- \approx N_+ \approx (k_3 t)^{-1}. \tag{15}$$

The ionization source can be related to the dose rate. Since one rad is defined as depositing 100 erg/g, and 34 eV are required to make one electron-ion pair, the relation is

$$S\left(\frac{\text{elect.}}{\text{cm}^3\ \text{s}}\right) = 2.2 \times 10^9 \left(\frac{\rho}{\rho_0}\right) \dot{D}\left(\frac{\text{rad}}{\text{s}}\right). \tag{16}$$

Here $\rho_0 = 1.23$ g/l is the density of sea level air. This relation assumes that all ionization is completed in times short compared with the variation of $\dot{D}$.

The *mobility* μ_e or μ_i of an electron or ion is defined as the ratio of its drift velocity to the electric field causing the drift. Typical values of the mobilities at sea level and their scaling with air density ρ are

$$\mu_e\left(\frac{\text{m}}{\text{s}}\right) \Big/ \left(\frac{\text{V}}{\text{m}}\right) \approx 0.3 \left(\frac{\rho_0}{\rho}\right)$$
$$\mu_i\left(\frac{\text{m}}{\text{s}}\right) \Big/ \left(\frac{\text{V}}{\text{m}}\right) \approx 2.5 \times 10^{-4} \left(\frac{\rho_0}{\rho}\right). \tag{17}$$

Small differences between the mobilities of various ions are usually neglected. The electron mobility is not independent of the electric field, and is effected by water vapor [7], [10].

Since the mobility of electrons is much larger than that of ions, electrons dominate the conductivity at early times when the densities of electrons and ions are comparable. In this circumstance the air conductivity is

$$\sigma = eN_e\mu_e \tag{18}$$

where $-e$ is the electron charge. Using (13) and other data stated above, we can relate the conductivity to the dose rate and find

$$\sigma\left(\frac{\text{mho}}{\text{m}}\right) \approx \frac{1 \times 10^{-4}}{(\alpha + k_1)} \dot{D}\left(\frac{\text{rad}}{\text{s}}\right). \tag{19}$$

This result is independent of air density except through the term k_1. It should be noted, however, that variation of the ionization completion time with ρ and the dependence of μ_e on E/ρ (E = electric field) make the result only approximate.

At late times, when the electrons are almost all attached in O_2^-, ion conductivity can dominate.

V. THE SPHERICALLY SYMMETRIC CASE

We now solve Maxwell's equations for the case in which the Compton current density **J** is radial, and J and σ are spherically symmetric. The radial current leads to an electric field **E**, which is also radial and spherically symmetric. Since the curl of such an **E** vanishes, no magnetic field **B** is produced according to the Maxwell equation

$$\frac{\partial \mathbf{B}}{\partial t} = -\nabla \times \mathbf{E} = 0. \tag{20}$$

The only nonvanishing Maxwell equation involves the radial components of **E** and **J**,

$$\epsilon_0 \frac{\partial E}{\partial t} + \sigma E = -J. \tag{21}$$

The solution of this ordinary first-order differential equation is easy to understand. At early times J and σ begin at arbitrarily small values, and then increase. Therefore, E also begins at arbitrarily small values. Thus at sufficiently early times, the term σE is negligible. In this regime, the solution of (21) is

$$E \approx \frac{1}{\epsilon_0} \int_{-\infty}^{t} J\, dt, \tag{22}$$

which indicates that J is charging up the capacitance of space. E will rise exponentially if J does. At some time, the conduction current σE may become comparable with the displacement current $\epsilon_0 \partial E/\partial t$. If after this time we neglect the latter, we obtain

$$E \approx -\frac{J}{\sigma} \equiv E_s. \tag{23}$$

From (4) and (19) we see that E_s is independent of $\dot{D}$ since J and σ are both proportional to $\dot{D}$. Thus E becomes constant at the *saturated* value E_s, and it is indeed a good approximation to neglect $\partial E/\partial t$.

From our estimates of J and σ we find

$$E_s \left(\frac{\mathrm{V}}{\mathrm{m}}\right) \approx 2 \times 10^{-4} (\alpha + k_1)(\mathrm{s}^{-1}). \tag{24}$$

With $\alpha = 2 \times 10^8$ (not atypical), this formula gives $E_s = 6 \times 10^4$ V/m at sea level where $k_1 = 1 \times 10^8$, and $E_s = 4 \times 10^4$ V/m at higher altitudes where k_1 is negligibly small compared with α.

After the gamma pulse and the Compton current reach their peaks, the value of α effectively goes to zero. Equation (24) then indicates that the E_s falls to about 2×10^4 V/m at sea level. The displacement current remains negligible, and E follows E_s. At sea level, within some kilometers from the nuclear burst, this value is maintained for some tens of microseconds, after which the dominance of ion conductivity causes E to fall gradually, approximately as $\sqrt{S}$. This behavior can be deduced from the approximate solution (14) and (4).

VI. EMP FROM SURFACE BURSTS

For a burst in the air just above the ground or ocean surface, the Compton current and conductivity in the air hemisphere are as described above, and a radial electric field is produced as in section V. However, soil conductivities are of the order of 10^{-2} mho/m, and the ocean conductivity is about 4 mho/m. These values are higher than the air conductivities over most of the EMP space-time source region. Thus the ground shorts out the radial electric field near it; as a result, magnetic and transverse electric fields are produced and a signal is radiated to great distances. We shall give here a somewhat qualitative discussion of the phenomena involved.

Much of the basic theory of EMP was developed in a series of lectures given by this author in 1963–1964 at AFWL, by invitation from Wallace D. Henderson. (This was at the beginning of an active and outstanding program on EMP at AFWL, fostered later by Donald Dowler and by John Darrah, under support from the U.S. Air Force and the Defense Nuclear Agency (DNA).) These lectures were written up in two LASL reports, one [11] dealing with surface bursts and the other [12] with high-altitude bursts. These reports have not been published in the open literature, due to specific nuclear weapon data contained therein. The present paper will make use of EMP physics developed in those reports.

The surface-burst EMP can be understood in terms of three phases. The first is the *wave phase* in which the conduction current is small compared with the displacement current. This phase corresponds to the time before saturation as described in Section V, and in it Maxwell's equations are approximately linear. The *diffusion phase* is entered at saturation when the conduction current exceeds the displacement current and the latter can be neglected. During this phase, the return conduction current (which, in the spherically symmetric case, tries to cancel the Compton current) shifts to the ground from the air just above it. Thus current loops are formed, and an azimuthal magnetic field is produced near the ground surface. This field diffuses up into the air and down into the ground, by the familiar *skin-effect* process. When the *skin depth* in the air reaches to an angular elevation of about 1 rad (referred to the burst point), the diffusion is completed and the final *quasi-static phase* is entered. During this phase the induction (transverse) part of the electric field is small compared with the electrostatic (longitudinal) part, and the Compton and conduction currents are approximately in steady balance.

The most convenient of the familiar units for discussing and computing the EMP are the CGS Gaussian units for the reasons that Maxwell's equations then explicitly display the speed of light, and that E and B are equal for a free wave in vacuum; these properties simplify the transformations of variables that turn out to be helpful. In this system electric fields and charges are in electrostatic units (ESU), and magnetic fields and currents are in electromagnetic units (EMU). The relation to MKS units

TABLE II
RELATION OF CGS GAUSSIAN AND MKS UNITS

Electric field	1 stat volt/cm = 3×10^4 volt/meter
Magnetic field	1 Gauss = 10^{-4} Weber/meter^2
Charge	1 stat-Coulomb = $(1/3)\times10^{-9}$ Coulomb
Current	1 ab-amp = 10 amperes
Conductivity	1 cm^{-1} = (10/3)mho/meter

is summarized in Table II. Maxwell's equations and the conservation of charge take the form (in air)

$$\frac{1}{c}\frac{\partial \mathbf{B}}{\partial t} = -\nabla \times \mathbf{E} \tag{25}$$

$$\frac{1}{c}\frac{\partial \mathbf{E}}{\partial t} + 4\pi\sigma\mathbf{E} + 4\pi\mathbf{J} = \nabla \times \mathbf{B} \tag{26}$$

$$\frac{1}{c}\frac{\partial \rho}{\partial t} + \nabla \cdot \mathbf{J}_T = 0. \tag{27}$$

Here ρ is the charge density, $\mathbf{J}$ is the Compton current density, and $\mathbf{J}_T = \mathbf{J} + \sigma\mathbf{E}$. In time varying problems, the two Maxwell equations (25) and (26) are sufficient to advance the fields. The other two Maxwell equations involving $\nabla \cdot \mathbf{B}$ and $\nabla \cdot \mathbf{E}$ are not needed; they follow automatically [13] from (25)-(27) provided they are satisfied initially, as they are if E, B, and ρ vanish initially. Furthermore, we do not need to solve (27) to find ρ, since ρ does not enter (25) and (26).

We use spherical coordinates r, θ, ϕ, right handed in that order, with polar angle θ measured from the upward vertical. Neglecting all asymmetries except the presence of a flat uniform ground, we shall have field components E_r, E_θ, and B_ϕ. Maxwell's equations become, in air

$$\frac{1}{c}\frac{\partial B_\phi}{\partial t} = -\frac{1}{r}\frac{\partial}{\partial r} rE_\theta + \frac{1}{r}\frac{\partial}{\partial \theta}E_r \tag{28}$$

$$\frac{1}{c}\frac{\partial E_\theta}{\partial t} + 4\pi\sigma E_\theta + 4\pi J_\theta = -\frac{1}{r}\frac{\partial}{\partial r} rB_\phi \tag{29}$$

$$\frac{1}{c}\frac{\partial E_r}{\partial t} + 4\pi\sigma E_r + 4\pi J_r = \frac{1}{r\sin\theta}\frac{\partial}{\partial \theta}\sin\theta B_\phi. \tag{30}$$

In the ground, the relative dielectric constant ϵ_g should multiply the first terms in the last two equations.

Because the Compton current source appears to move outward with speed c, we have found it convenient [14] for treating the early-time problem to introduce the retarded time (in length units) τ and *outgoing* and *ingoing* fields F and G:

$$\tau = ct - r \tag{31}$$

$$F = r(E_\theta + B_\phi), \quad E_\theta = (F+G)/2r$$

$$G = r(E_\theta - B_\phi), \quad B_\phi = (F-G)/2r. \tag{32}$$

Maxwell's equations then take the form

$$\frac{\partial F}{\partial r} + 2\pi\sigma F = -4\pi r J_\theta + \frac{\partial E_r}{\partial \theta} - 2\pi\sigma G \tag{33}$$

$$\frac{\partial G}{\partial \tau} + \pi\sigma G = \frac{1}{2}\frac{\partial G}{\partial r} - 2\pi r J_\theta - \frac{1}{2}\frac{\partial E_r}{\partial \theta} - \pi\sigma F \tag{34}$$

$$\frac{\partial E_r}{\partial \tau} + 4\pi\sigma E_r = -4\pi J_r + \frac{1}{2r^2\sin\theta}\frac{\partial}{\partial \theta}[\sin\theta(F-G)]. \tag{35}$$

Note that (33) for F contains no time derivatives, a consequence of the fact that a constant phase point on an outgoing wave maintains a constant retarded time. Thus F is obtained by integrating (33) in r, whereas G is obtained by integrating (34) in τ. Now, at early times, the range of τ integration is c times a few tens of nanoseconds or a few meters, while the range of r integration is of the order of the gamma absorption length or a few hundred meters. Therefore, the ingoing field G is small compared with the outgoing field F at early times, and G can be neglected. Also, in the wave phase, the conduction current is small compared with the displacement current when

$$\sigma \ll \frac{\alpha}{4\pi c}\ \text{cm}^{-1} \approx 10^{-3}\ \text{mho/m}. \tag{36}$$

Thus the σE_r term may be dropped from (35). Further, since at early times J_θ is small compared with J_r, the wave phase equations become

$$\frac{\partial F}{\partial r} + 2\pi\sigma F = \frac{\partial E_r}{\partial \theta} \tag{37}$$

$$\frac{\partial E_r}{\partial \tau} = -4\pi J_r + \frac{1}{2r^2}\frac{\partial F}{\partial \theta}. \tag{38}$$

Here we have put $\sin\theta = 1$, since F is confined to angles θ close to $\pi/2$ near the ground surface.

Note that we have retained the σF term in (37). As first noticed by Bergen R. Suydam of LASL, the wave phase further subdivides into two parts depending on whether

$$\sigma \lesssim \frac{1}{2\pi\lambda_a}\ \text{cm}^{-1} \approx 2\times10^{-5}\ \text{mho/m}. \tag{39}$$

When σ is less than this value, the σF term may be dropped and we find

$$\frac{\partial}{\partial \tau}\frac{\partial F}{\partial r} = -4\pi\frac{\partial J_r}{\partial \theta} + \frac{1}{2r^2}\frac{\partial^2 F}{\partial \theta^2}. \tag{40}$$

This equation shows that the source of the transverse field F is at the ground surface where J_r drops to zero in going from air to ground. The equation is linear, so that F (and E_r) will rise exponentially if J_r does. This phase is therefore called the α wave phase. Assuming that all quantities rise as $\exp(\alpha\tau/c)$, we

reduce (40) to

$$\frac{\partial F}{\partial r} = -\frac{4\pi c}{\alpha}\frac{\partial J_r}{\partial \theta} + \frac{c}{2\alpha r^2}\frac{\partial^2 F}{\partial \theta^2}. \tag{41}$$

This equation has the form of a diffusion equation, which may seem odd considering that conductivity has been totally neglected. What is happening is that F, produced very near the ground surface, is spreading upward by *diffraction* as it propagates outward.

Equation (40) shows an interesting feature of the retarded time equations, which is troublesome for numerical calculations. If we Fourier analyze F in r, $z \approx r(\pi/2 - \theta)$, and τ, we find from the homogeneous form of (40),

$$\omega k_r = \frac{1}{2} k_z^2. \tag{42}$$

Thus the frequency ω is infinite for finite wavenumber k_z when k_r vanishes. Because of this, well-centered explicit difference equations constructed from (33)–(35) are unconditionally unstable. Robert D. Richtmyer showed how to construct stable equations using implicit differencing in the θ (or z) direction [14].

When σ exceeds the value in (39) but is still less than that in (36), we may drop the term $\partial F/\partial r$ in (37) and find

$$\frac{\partial E_r}{\partial \tau} = -4\pi J_r + \frac{1}{4\pi\sigma r^2}\frac{\partial^2 E_r}{\partial \theta^2}. \tag{43}$$

This is another diffusion type of equation, although we are still in the wave phase, and the conduction current is still small compared with the displacement current. However, the outgoing field F, which must travel a distance comparable to λ_a to get out, is being attenuated and limited by conductivity.

The solutions of (40) and (43) are discussed and compared with computer calculations in a forthcoming textbook [15] on surface-burst EMP. The transverse field E_θ peaks at the end of the wave phase at a value comparable with the saturated field E_s in (24). The magnetic field B_ϕ peaks later, in the diffusion phase. Within a few kilometers from the burst, E_θ and B_ϕ are confined to angles of a few degrees above the ground during the wave phase. Most of the air volume sees only the radial E of Section V.

In the diffusion phase, it is simplest to return to the real-time equations (28)–(30). When σ is large compared with the value in (36), the displacement current terms can be dropped. Angular derivative terms can be shown to be larger than radial derivative terms, and E_r is more important than E_θ. Equations (28) and (30) then reduce to

$$\frac{1}{c}\frac{\partial B_\phi}{\partial t} = \frac{\partial}{\partial z}\left(\frac{J_r}{\sigma}\right) + \frac{1}{4\pi}\frac{\partial}{\partial z}\frac{1}{\sigma}\frac{\partial B_\phi}{\partial z}. \tag{44}$$

Here we have introduced the vertical coordinate $z \approx r(\pi/2 - \theta)$ since the magnetic field is confined to points near the ground surface. This is the standard diffusion equation of the skin effect, and it can be solved under various assumptions for the time dependence of σ. Note that $-J_r/\sigma$ is the saturated field E_s, which is approximately constant in time. By integrating (44) over z, one finds that the total magnetic flux

$$\Phi \equiv \int B_\phi \, dz \tag{45}$$

increases with time according to

$$\frac{1}{c}\frac{\partial \Phi}{\partial t} = -E_s, \qquad \Phi = -c\int E_s \, dt \approx -c\Delta t E_s \tag{46}$$

where Δt is the time after saturation. This result can be used to estimate the value B_0 of B_ϕ at the ground surface and the skin depth δ in the air. From the relations

$$B_0 \approx 4\pi J_r \delta \qquad \Phi \approx B_0 \delta \approx 4\pi J_r \delta^2 \tag{47}$$

we find by comparison with (46)

$$\delta \approx \sqrt{\frac{c\Delta t}{4\pi\sigma}} \qquad B_0 \approx -\sqrt{4\pi\sigma c\Delta t}\, E_s. \tag{48}$$

The peak B_ϕ, which occurs near the peak of the gamma pulse and Compton current, can be estimated by putting the value of σ at that time in (48). Note that the peak B_ϕ varies only as the square root of the peak gamma flux since E_s is roughly constant.

The derivation of (47) and (48) has assumed that the conductivity of the ground is large compared with that of the air. At positions very close to a nuclear burst, the opposite of this assumption is true near the peak of the Compton current. In this case, B_0 would limit at approximately the value obtained by using the ground conductivity σ_g for σ in (48). Richard Schaefer and William Graham of Research & Development Associates, Inc. (RDA) have pointed out [16] that the Compton current in the top layers of the ground (10 cm or so) must be taken into account in this case and can result in a reversed B_ϕ near the ground surface and near the peak of the Compton current pulse.

After the peak of the gamma flux, J drops, but the skin depth increases as

$$\delta^2 \approx \int \frac{c\,dt}{2\pi\sigma}. \tag{49}$$

The result is that B_ϕ at the ground surface does not decrease much during the remainder of the diffusion phase.

In the quasi-static phase, the divergence of the total current density must vanish and $\mathbf{E}$ must be derivable from a potential ϕ. Thus ϕ must satisfy

$$\nabla \cdot (\sigma \nabla \phi) = \nabla \cdot \mathbf{J}. \tag{50}$$

This author showed [11] that the solution of this problem is such that the electric field and the conduction current are very nearly in the θ direction. Thus while the Compton current

flows outward radially, the return conduction current flows down to the ground in the θ direction. This result, together with formulas like (1) for the Compton current, can be used directly to estimate E_θ and B_ϕ. E_r is small in this phase. The result also accounts for the shape and orientation of curved lightning strokes in the θ direction that have been photographed in nuclear tests [17]. It may not account for the existence of the strokes, for the fields are believed to be only of the order of 3×10^4 V/m. This author has suggested that the strokes may involve initially only detachment of electrons from O_2^- rather than ionization of neutral atoms; the former requires considerably less energy.

While it is possible to understand the behavior of the EMP by analytical methods such as those above, for system applications it is more practical to calculate detailed results using computer codes such as LEMP [14] and SUBL, developed by Mission Research Corporation (MRC) for DNA. LEMP is a retarded-time code that calculates to several tens of μs. SUBL, a real-time code, then takes over and calculates to times of the order of 0.1 s. A code SCX similar to LEMP has been developed and applied by AFWL.

We have not discussed here the EMP problem in the ground, which is dominated by conductivity. Soil conductivities and permittivities typically vary substantially with frequency and with water content of the soil. Methods for treating this problem were developed by Longmire and Longley [18] and by Longmire and Smith [19]; the soil is modeled as an RC network in which the resistances depend on water content.

VII. EMP FROM HIGH ALTITUDE BURSTS

For a nuclear burst well above the atmosphere, let us say at altitudes of 100 km or more, the prompt gammas are far more intense than any other component. After emission from the nuclear device, the prompt gammas lie in a spherical shell with thickness of a few meters and with a radius which increases at the speed of light. The downward going part of this shell begins to interact appreciably with the atmosphere at altitudes of 40-50 km. At about 30 km, the gammas have passed through a mass of air equivalent to one absorption length, and the absorption length is approximately equal to the atmospheric *scale height* (about 7 km). At this altitude the Compton recoil current is at maximum, for at higher altitudes there is less air density to scatter the gammas, and at lower altitudes the gammas have been mostly absorbed.

The Compton current has two components. First, the component in the direction radial from the burst produces principally a radial electric field, as in Section V. However, since only part of the gamma shell intersects the atmosphere we do not have complete spherical symmetry. Thus some transverse fields, principally of *electric dipole* type, are generated by the radial current. Second, the geomagnetic field causes the Compton current to have a transverse component perpendicular to the radial direction. This component directly generates outgoing and ingoing transverse fields, principally of *magnetic dipole* type.

The outgoing magnetic dipole EMP is a short pulse of high amplitude, owing to the fact that the Compton current pulse moves outward in synchronism with this part of the EMP. The electric dipole EMP is a long pulse of lower amplitude since a radial current element radiates no fields in the radial direction; the electric dipole fields are radiated at angles off the radial direction, and therefore fall behind the gamma and Compton current shell.

The outgoing magnetic dipole EMP was discovered experimentally in the U.S. nuclear test series in 1962. Only the electric dipole part had been predicted, and some measurements were overdriven. However, Richard Wakefield of LASL obtained reliable data. The explanation of the data in terms of the outgoing magnetic dipole effect was first given by this author [12] in 1963 in his EMP lectures at AFWL.

There has been a good deal of misunderstanding about various aspects of high altitude EMP. In order to make the basic phenomena as clear as possible, we shall first imagine a flat earth with a flat exponential atmosphere, with a planar pulse of gamma rays approaching it from the vertical direction. Let the vertical coordinate z increase downward, i.e., z is essentially the same as the radial coordinate from the burst, which is imagined to be very far away. Let the geomagnetic field be in the y direction so that the Compton current will have components J_z and J_x. (The coordinates x, y, and z are right handed and Cartesian.) We shall have field components E_z, E_x, and B_y, which depend only on z and t.

Maxwell's equations, again in Gaussian units, become

$$\frac{1}{c}\frac{\partial B_y}{\partial t} = -\frac{\partial}{\partial z}E_x \tag{51}$$

$$\frac{1}{c}\frac{\partial E_x}{\partial t} + 4\pi\sigma E_x + 4\pi J_x = -\frac{\partial}{\partial z}B_y \tag{52}$$

$$\frac{1}{c}\frac{\partial E_z}{\partial t} + 4\pi\sigma E_z + 4\pi J_z = 0. \tag{53}$$

We again transform to retarded time τ and outgoing and ingoing fields F and G

$$\tau = ct - z \tag{54}$$

$$F = E_x + B_y, \qquad E_x = (F+G)/2,$$

$$G = E_x - B_y, \qquad B_y = (F-G)/2. \tag{55}$$

Under the retarded-time transformation, the partial derivatives are replaced by

$$\frac{1}{c}\frac{\partial}{\partial t} \rightarrow \frac{\partial}{\partial \tau}$$

$$\frac{\partial}{\partial z} \rightarrow \frac{\partial}{\partial z} - \frac{\partial}{\partial \tau} \tag{56}$$

and (51)-(53) become

$$\frac{\partial F}{\partial z} + 2\pi\sigma F = -4\pi J_x - 2\pi\sigma G \tag{57}$$

$$\frac{\partial G}{\partial \tau} + \pi\sigma G = \frac{1}{2}\frac{\partial G}{\partial z} - 2\pi J_x - \pi\sigma F \tag{58}$$

$$\frac{\partial E_z}{\partial \tau} + 4\pi\sigma E_z = -4\pi J_z. \tag{59}$$

Notice that the radial electric field E_z is not coupled to the other fields in this case of planar symmetry. Equation (53) or (59) has the same form as (21), only in different units. The nature of the solution is the same as discussed in Section V. At early times, E_z is proportional to the time integral of J_z. If the total charge displacement is sufficient, E_z saturates at the value $-J_z/\sigma$. The condition that saturation be reached before the peak of the Compton current pulse (again assumed to rise like $\exp(\alpha t)$) is that the peak conductivity reach the value

$$\sigma \geqslant \frac{\alpha}{4\pi c}\ \text{cm}^{-1} \approx 10^{-3}\ \text{mho/m}. \tag{60}$$

Here we have used $\alpha \approx 10^8$/s. Using (19) as an estimate we find that dose rates of about 10^9 rads/s are needed to produce saturation of the radial electric field. For a nominal 1-megaton burst, saturation would occur only within slant distances of about 50 km between the burst point and the EMP source region. We shall see that it is much easier to saturate the outgoing field F.

Let us assume that, as will be verified below, G is small compared with F so that the σG term in (57) can be neglected. Then the difference between the equations for F and E_z is that E_z is integrated in τ at fixed z, while F is integrated in z at fixed τ. Equation (57) says that the value of F at a given retarded time is built up by the source term $-4\pi J_x$, and attenuated by the conduction term $2\pi\sigma$F as the F wave enters the atmosphere (increasing z). At altitudes above 30 km, where attenuation of the gammas is not significant, both J_x and σ increase as $\exp(z/h)$ where h is the atmospheric scale height. Thus at sufficiently high altitudes the σF term in (57) will also be negligible, and the solution is

$$F(z, \tau) \approx -4\pi \int_{-\infty}^{z} J_x(z', \tau)\, dz' \approx -4\pi h J_x(z, \tau). \tag{61}$$

However if σ becomes large enough, F will saturate at the value

$$F = -2J_x/\sigma. \tag{62}$$

Saturation occurs when the value from (61) exceeds the saturated value, or when

$$\sigma \geqslant \frac{1}{2\pi h}\ \text{cm}^{-1} \approx 10^{-6}\ \text{mho/m}. \tag{63}$$

This is much smaller than the value (60) needed to saturate E_z. From the ratio of the values (60) and (63) we see that the transverse field will saturate at distances some thirty times farther from a burst than the radial field, or up to 1500 km for a nominal 1-megaton burst.

The reason F is more easily saturated than E_z is that F integrates J_x over a scale height, while E_z integrates J_z over the rise time multiplied by c. The latter distance is of the order of a few meters, while the former is about 7 km. It is for the same reason that G is small compared with F; (58) shows that G integrates J_x in time. Note also that once F saturates, the source term $2\pi J_x + \pi\sigma F$ effectively vanishes in the G equation. In this regime the outgoing wave F induces a conduction current which effectively cancels J_x, leaving no net current to drive ingoing waves.

The smallness of G compared with F implies, according to (55), that

$$E_x \approx B_y \qquad F \approx 2E_x, \tag{64}$$

and that (57) is approximately

$$\frac{\partial E_x}{\partial z} + 2\pi\sigma E_x = -2\pi J_x(z, \tau). \tag{65}$$

This equation, derived by this author [12] in the AFWL lectures and called the *outgoing wave approximation*, is the basic equation of high altitude EMP theory. In MKS units it reads

$$2\frac{\partial E_x}{\partial z} + Z_0\sigma E_x = -Z_0 J_x \tag{65'}$$

where $Z_0 = \sqrt{\mu_0/\epsilon_0} \approx 377\ \Omega$ is the impedance of space. In spherical geometry, i.e., for a point rather than planar source of gammas, the derivative with respect to z is replaced by

$$\frac{\partial}{\partial z} \to \frac{1}{r}\frac{\partial}{\partial r}\, r \tag{66}$$

as was first shown by Karzas and Latter [20]. Thus (65') becomes

$$2\frac{\partial}{\partial r}(rE_t) + Z_0\sigma(rE_t) = -Z_0(rJ_t). \tag{67}$$

Here J_t and E_t are the components transverse to the radial coordinate r (measured from the burst point). This equation is the same as (65') except that rJ_t and rE_t have replaced J_x and E_x. When the source region is thin compared with r the planar approximation is sufficient in the source region, but one should remember that the EMP amplitude will fall as $1/r$ eventually.

The behavior of the solution of (65) for E_x is the same as that discussed above for F. For a given retarded time τ, E_x increases as $\exp(z/h)$ at very high altitudes. If the source is sufficiently strong, E_x will saturate at

$$E_x = -\frac{J_x}{\sigma} \equiv E_s \approx 1\ \text{ESU} = 3 \times 10^4\ \text{V/m}. \tag{68}$$

E_x will then remain saturated until the wave reaches an altitude below 30 km where, due to absorption of the gammas, both σ and J_x fall away. Below this altitude, called the altitude of *desaturation*, (65) indicates $\partial E_x/\partial z \approx 0$, or $E_x \approx$ constant;

the EMP propagates as a free wave. Actually, of course, E_x will fall as $1/r$. Desaturation occurs at that altitude at which σ falls below

$$\sigma \leqslant \frac{1}{2\pi\lambda_s} \text{ cm}^{-1}$$

$$\leqslant \frac{2}{Z_0\lambda_s} \text{ mho/m.} \tag{69}$$

Here λ_s in centimeters or meters, respectively, is the scattering length of the gammas at that altitude. (Note that scattered gammas quickly fall far behind the shell of unscattered gammas, and contribute insignificantly to the main EMP.)

At arbitrarily early retarded times J_x and σ are arbitrarily small, and saturation does not occur at all. The rise of the final EMP is similar to the rise of the Compton current, before saturation. The duration of the final EMP is not longer than the duration of the Compton current pulse at the desaturation altitude.

Critics of high altitude EMP theory have often been confused about the effect of diffraction on the final EMP (i.e., below the source region) principally because they try to calculate the EMP as a Huyghens integral over the source. From the differential equation approach presented here, it is clear that the diffraction effect is due to the fact that the source current does not form a complete spherical magnetic dipole current; only that part of the shell intersecting the atmosphere but not yet absorbed is present. It is also clear that diffraction will have no effect on the EMP until such retarded times that signals can arrive at the observer from the edge of the source current region. In this way, this author showed [12] that diffraction has negligible effect on the EMP in most cases of practical interest.

Others have tried to calculate the EMP as the sum of the cyclotron radiations of individual Compton recoil electrons. In this approach it is more difficult to take the air conductivity into account. The density of Compton recoil electrons is usually amply high to justify the continuum approach used above.

Historically, the existence of geomagnetically induced transverse currents was considered before 1962. In 1960, Karzas and Latter [21] and this author (unpublished) studied the pushing out of the geomagnetic field near a low-altitude burst. Karzas and Latter found the expression for the saturated transverse electric field, but the radiated pulse was not considered in their early work. These two authors, particularly William J. Karzas, have contributed greatly in the development of EMP theory, in carrying it to system applications, and in defending it against critics with limited understanding of EMP but strong influence.

The high-altitude EMP is well understood in terms of the theory outlined above. For system applications it is more practical to use computer codes such as the MRC-DNA code CHAP, which is also self-consistent and includes both outgoing and ingoing fields [3], or the codes HEMP and HEMP-B developed by AFWL. Notable contributions to calculation techniques were made by John H. Erkkila of AFWL, Charles N. Vittitoe of Sandia Corporation, and William T. Wyatt of Harry Diamond Laboratories.

VIII. GEOMAGNETIC EMP FROM LOW ALTITUDE BURSTS

The theory of Section VII also applies at early times to air bursts at low altitudes. Here the desaturation radius is no more than a few kilometers from the burst, and the air density can be treated as constant. Assume a gamma pulse rising as $\exp(\alpha\tau/c)$. The desaturation radius R is determined by (69), which on consideration of the gamma attenuation leads to a relation between R and τ

$$\frac{1}{R^2} \exp\left(\frac{\alpha\tau}{c} - \frac{R}{\lambda_s}\right) \approx \text{constant}$$

or

$$R \approx \frac{\alpha\lambda_s}{c}\tau - 2\lambda_s \ln R + \text{constant.} \tag{70}$$

Thus the desaturation radius increases approximately linearly with τ. Since the signal at great distance r is given by

$$E(r) \approx E_s \frac{R}{r}, \tag{71}$$

and since E_s is constant, the radiated signal rises approximately linearly in time for an exponentially rising gamma source. The linear rise rate is proportional to α. These results were developed by this author in a lecture [22] to the VELA Summer Study in 1965. It should be noted that the magnetic dipole EMP has smaller amplitude at lower altitude, and is followed by an electric dipole EMP due to the air density gradient.

IX. EARLY HISTORY OF EMP IN THE U. S.

Enrico Fermi suggested that there would be electromagnetic effects in the first nuclear explosion in 1945. It is not recorded what mechanism he had in mind, but it would be surprising if he missed the Compton recoil mechanism. Some failures of instrumentation on the first test were attributed to EMP. By 1952, first attempts were being made by LASL to use radiated EMP as a diagnostic indicator of the nuclear reaction history. In 1954, Richard L. Garwin of LASL estimated [23] the EMP that would be radiated by an asymmetric gamma source in the exponential phase of the signal; his results agree with later, more detailed treatments. In 1956, Peter H. Haas led a group from the Diamond Ordnance Fuse Laboratory in making magnetic field measurements near nuclear tests in Nevada; their interest was in the possible detonation of magnetic mines. Since 1960, beginning with the Minuteman missile system, military system developers have considered the potential impact of EMP on their systems.

The development of EMP theory and computer codes has been supported principally by LASL, AFWL, and DNA. In the latter agency, the contributions of Peter Haas in fostering EMP

research and applications over many years since the beginning of the efforts in this area have been absolutely essential for the progress which has been achieved.

OUTSTANDING CONTRIBUTORS

John S. Malik of the Los Alamos Scientific Laboratory (LASL) has provided information and guidance on gamma sources to this author and his colleagues since the beginning of our EMP efforts in 1960. Monte Carlo calculations of gamma and neutron transport were performed at LASL under the guidance of Malik, and at AFWL under Richard Schaefer.

Bergen R. Suydam has contributed much to the understanding of surface burst EMP, and of the EMP from air bursts, which is controlled by the vertical gradients in air and water vapor density. The principal efforts in developing the MRC computer codes were provided by this author's colleagues H. Jerry Longley and, in recent years, Robert M. Hamilton. The AFWL program of codes and applications was upheld by the outstanding work of Carl E. Baum, William R. Graham, Richard R. Schaefer, Gerard K. Schlegel, William A. Radasky, Michael A. Messier, William E. Page, and others.

REFERENCES

[1] R. D. Evans, *The Atomic Nucleus.* New York: McGraw-Hill, 1955.

[2] C. L. Longmire and H. J. Longley, Improvements in the Treatment of Compton Current and Air Conductivity in EMP Problems, Defense Nuclear Agency, Report DNA-3192T, October 1971.

[3] H. J. Longley and C. L. Longmire, Development of the CHAP EMP Code, Defense Nuclear Agency, Report DNA-3150T, January 1972, unpublished.

[4] G. R. Knutson, Air Force Weapons Laboratory, private communication. See also EMP Theoretical Note 161, February 1972, and Theoretical Note 204, September 1973.

[5] J. P. Vajk, Critique of Compton Current Models Used in High Altitude EMP Computer Codes, Lawrence Livermore Laboratory, Report UCRL-77860, December 1975.

[6] C. L. Longmire and J. Koppel, Formative Time Lag of Secondary Ionization, Mission Research Corporation, Report MRC-R-88, January 1974.

[7] C. E. Baum, Electron Thermalization and Mobility in Air, EMP Theoretical Note 12, July 1965.

[8] A. V. Phelps, *Can. J. Chem.*, vol. 47, pg. 1783, 1969.

[9] Defense Nuclear Agency, *Reaction Rate Handbook,* DNA-1948H, March 1972.

[10] W. T. Wyatt, Computed Electron Drift Velocity in Moist Air, U. S. Army Eng. Research and Dev. Lab., Report 1890, (Theoretical Note 182), March 1967.

[11] C. L. Longmire, Close-In E. M. Effects Lectures I through IX, Los Alamos Scientific Lab., Report LAMS-3072, April 1964, unpublished.

[12] —, Close-In E. M. Effects Lectures X and XI, Los Alamos Scientific Lab., Report LAMS-3073, April 1964, unpublished.

[13] —, Elementary Plasma Physics. New York: Wiley, 1963, pg. 3.

[14] H. J. Longley and C. L. Longmire, Development and Testing of LEMP 1, Los Alamos Scientific Lab., Report LA-4036, December 1969.

[15] C. L. Longmire, Theory of the EMP from Nuclear Surface Bursts, in preparation for the Defense Nuclear Agency.

[16] W. R. Graham, R. R. Schaefer, and W. Pine, "New Considerations in Close-In EMP," the RAND Corporation, RM-6208-PR, January 1970; also listed by Air Force Weapons Laboratory as AFWL-TR-70-27, September 1970, unpublished.

[17] M. A. Uman, D. F. Seacord, G. H. Price, and E. T. Pierce, *J. Geophys. Res.*, vol. 77, pg. 1591, 1972.

[18] C. L. Longmire and H. J. Longley, Time Domain Treatment of Media with Frequency-Dependent Electrical Parameters, Defense Nuclear Agency, Report DNA-3167F, March 1971.

[19] —, and K. S. Smith, A Universal Impedance for Soils, Defense Nuclear Agency, Report DNA-3788T, October 1975.

[20] W. J. Karzas and R. Latter, *Phys. Rev.*, vol. 137B, pg. 1369, 1965.

[21] —, and R. Latter, *J. Geophys. Res.*, vol. 67, pg. 4635, 1962.

[22] A. M. Peterson and J. F. Vesecky, Project VELA Summer Study 1965 on EMP, Stanford Res. Inst., Report No. Project 5563, March 1967, unpublished.

[23] R. L. Garwin, Determination of Alpha by Electro-magnetic Means, Los Alamos Scientific Lab., Report LAMS-1871, September 1954, unpublished.